Journal of Experimental and Clinical Application of Chinese Medicine

ORIGINAL RESEARCH

Open Access

The Tanshinones of *Salvia miltiorrhiza* Bunge Suppress GES-1 Apoptosis via Inhibiting EGFR-STAT3 Signaling Pathway *in vitro*

Yujia Weng [1,2], Hanlei Huang [1], Liping Han [1], Zhaohuan Lou [1,3,*]

1. School of Pharmaceutical Sciences, Zhejiang Chinese Medical University, 310053 Hangzhou, Zhejiang, China
2. Center for Drug Safety Evaluation and Research, College of Pharmaceutical Sciences, Zhejiang University, 310053 Hangzhou, Zhejiang, China
3. Zhejiang Provincial Key Laboratory of Pharmacology Research on TCM Treatment of Hypertension and related diseases, 310053 Hangzhou, Zhejiang, China

DOI: https://doi.org/10.62767/jecacm602.6554

Keywords

Tanshinone

EGFR-STAT3 signaling pathway

Chronic atrophic gastritis

Network pharmacology

* **Correspondence**

Zhaohuan Lou

School of Pharmaceutical Sciences, Zhejiang Chinese Medical University, 310053 Hangzhou, Zhejiang, China; Zhejiang Provincial Key Laboratory of Pharmacology Research on TCM Treatment of Hypertension and related diseases, 310053 Hangzhou, Zhejiang, China

E-mail: zhaohuanlou@zcmu.edu.cn

Received: 14 January 2025

Revised: 27 February 2025

Accepted: 16 April 2025

Published: 23 May 2025

Journal of Experimental and Clinical Application of Chinese Medicine 2025; 6(2): 1-18.

Abstract

Aim: Chronic atrophic gastritis (CAG), a precancerous lesion of gastric cancer. Current therapies face challenges including drug resistance and incomplete efficacy. Tanshinones exhibit anti-inflammatory and anti-tumor properties, yet their role in CAG remains unexplored. The present study aimed to explore the therapeutic effect and underlying mechanism of tanshinones on N-methyl-N′-nitro-N-nitrosoguanidine (MNNG)-induced CAG *in vitro*. **Methods:** The active tanshinones were screened from CNKI, PubMed and TCMSP databases. The CAG-related targets were collected from GeneCards database. Cytoscape 3.9.0 software was used to construct a compound-target network. A protein-protein interaction (PPI) network was constructed using a string database. The potential mechanism was analyzed by Gene Ontology (GO) and Kyoto Encyclopedia of Genes and Genomes (KEGG) pathway enrichment. Molecular docking was completed by Autodock software. An *in vitro* CAG model was established using the human gastric epithelial cell line GES-1, induced by MNNG. Cell viability of GES-1 was measured by Cell Counting Kit-8 (CCK-8) assay. TUNEL assay was used to evaluate cell apoptosis and protein expression of Epidermal growth factor receptor (EGFR), Signal transducer and activator of transcription 3 (STAT3) etc was determined by Western blot. **Results:** The compound-target network analysis found 12 active tanshinones and 42 common targets. The key targets were Cysteinyl Aspartate-specific Proteinase-3 (Caspase-3 (CASP3)), EGFR, STAT3, PTGS2, MMP2, ERBB2, and PPARG. Through enrichment analysis, 656 GO terms were enriched, whereas the top 15 pathways, including proteoglycans in cancer and apoptosis, were identified. Through molecular docking, cryptotanshinone, tanshinone IIA, dihydrotanshinone I, and tanshinone I were found to be stably bound to EGFR and STAT3. *In vitro* experiments indicated that tanshinones could significantly inhibit MNNG-induced GES-1 cell apoptosis, and markedly lower the protein expression of EGFR, STAT3, and Caspase-3. **Conclusion:** Tanshinones combination exhibited a positive effect on anti-CAG induced by MNNG *in vitro*, and this function is correlated with the suppression of EGFR-STAT3 signaling pathway and cell apoptosis.

1 Introduction

Chronic atrophic gastritis (CAG) is one of the most prevalent chronic digestive system illnesses characterized by both intrinsic gland atrophy and chronic inflammation of the stomach mucosa, and often accompanied by intestinal metaplasia or atypical hyperplasia. The common symptoms of CAG found in clinical are upper abdominal pain, fullness, belching, loss of appetite, weight loss, and anemia [1]. Multiple risk factors promote the development of CAG, including helicobacter pylori (Hp) infection and gastric autoimmunity [2]. It has been revealed that gastric cancer (GC) is a multi-stage process, which includes chronic gastritis, atrophy, intestinal metaplasia, and dysplasia [3], and CAG is a precancerous lesion of GC. Improving and/or curing CAG can effectively block the occurrence and development of GC. At present, antibiotic regimen for Hp and drugs for gastric protection are the main treatments for CAG [4]. Clinically, traditional Chinese medicine (TCM) has advantages in improving the symptoms of patients and delaying or even reversing the further development of CAG [5]. However, complete eradication of CAG is still a challenge due to its complex pathogenesis.

Salvia miltiorrhiza Bunge (*S. miltiorrhiza*, Danshen) is a well-known traditional Chinese herb and has been used in clinical for thousands of years. It possess functions on blood circulation-enhancing and blood stasis-removal, and used to treat cardiovascular disorders, such as coronary heart disease [6]. In *Salvia miltiorrhiza*, there is a class of lipophilic diterpenoid tanshinone, such as tanshinone IIA, cryptotanshinone, tanshinone I, and dihydrotanshinone I, which exert significant effects on anticancer, anti-inflammation, and antioxidant [7]. A number of studies indicated that tanshinones extracted from *S. miltiorrhiza* inhibited a variety of cancers both *in vitro* and *in vivo* models [8-10]. Our previous studies also have found that a diterpenoid tanshinones extract could significantly induce lung cancer cellline's apoptosis [11]. It has been reported that tanshinones play an important role in inhibiting inflammatory response [12], and tanshinone IIA exhibited a notable protective effect against inflammatory colitis [13]. Notably, tanshinones have shown direct anti-gastric cancer effects. For instance, diterpenoid tanshinones suppressed gastric cancer angiogenesis by modulating the PI3K/Akt/mTOR signaling pathway [14], while tanshinone IIA triggered ferroptosis in gastric cancer cells via p53-mediated down-regulation of SLC7A11 [15]. Meanwhile, compared with the single active compound, a combination of tanshinones separated from *S. miltiorrhiza* was found significantly enhanced the activities in inhibiting inflammation and retarding tumor progression [16]. It could alleviate colorectal tumorigenesis by inhibiting intestinal inflammation [17]. As CAG is an inflammatory disease and a precancerous lesion of GC, we speculated that tanshinones may also have potential therapeutic effects in CAG. In previous study, we separated an effective section in which containing tanshinones from *S. miltiorrhiza*, and have found that tanshinone IIA, cryptotanshinone, tanshinone I, and dihydrotanshinone I are the four main effective components [18]. In our previous pilot study, we found that the combination of tanshinones had better anti-lung cancer effect than single component [19]. So, in this study, we formed two tanshinones combinations (DST1, a combination of cryptotanshinone and dihydrotanshinone I; DST2, a combination of tanshinone IIA, cryptotanshinone, tanshinone I, and dihydrotanshinone I) according to the ratio in the active section we had separated, and tried to explore their effects on anti CAG *in vitro*, and to unveil the potential mechanisms.

Network pharmacology is a discipline based on the theory of systems biology, which analyzes the network

of biological systems and selects specific signal nodes for multi-target drug molecule design [20]. By constructing a drug-target-disease relationship through network data analysis, it may provide an effective way to reveal the possible molecular mechanisms of drug on therapy diseases [21]. Network pharmacology combined experiments verification is also an effective method to predict the complex mechanisms of TCM formulation [22] and their active ingredients [23]. In this study, we hope to unveil some potential mechanisms of the tanshinones combinations on anti CAG based on network paharmacology analysis and an *in vitro* CAG model [24], and try to offer some clues for the subsequent experimental research.

2 Materials and methods

2.1 Network pharmacology

2.1.1 Screening of active components

To identify the major tanshinones of *S. miltiorrhiza*, a literature search was conducted utilizing the CNKI and PubMed databases. The tanshinones from *S. miltiorrhiza* were searched by the Traditional Chinese Medicine Systems Pharmacology Database and Analysis Platform (TCMSP, https://tcmspw.com/tcmsp.php). The tanshinones with drug-likeness (DL)⩾0.18 and oral bioavailability (OB) ⩾30% were filtered out in accordance with TCMSP standards [25].

2.1.2 Target prediction of tanshinones

The structures or SMILES numbers of candidate tanshinones were obtained from PubChem (https://www.ncbi.nlm.nih.gov/). The targets of compounds were predicted and filtered through Swiss Target Prediction (http://www.swisstargetprediction.ch/). The obtained targets were transformed into common gene names via the Uniprot database (https://www.uniprot.org/) with the species selection of Homo sapiens. Cytoscape 3.9.0 (https://cytoscape.org/download.html) was used to create the compound-target network. The compounds and targets were denoted by various nodes. The correlation between the two nodes was represented by edges.

2.1.3 Collection of tanshinone targets for CAG therapy

The targets of CAG were obtained by searching the GeneCards human gene database (https://www.genecards.org/) with the term "chronic atrophic gastritis". Tanshinones and CAG common targets were derived from Venny 2.1.0 (http://bioinfogp.cnb.csic.es/tools/venny/index.html) .

2.1.4 Construction of protein-protein interaction (PPI) network

PPI analysis was performed using the STRING database (https://string-db.org/) of input common targets with the settings of Homo sapiens. Then, a PPI network diagram was obtained and exported in tsv format before being loaded into Cytoscape3.9.0 software for visual analysis. Eventually, the top 7 key genes were screened from the PPI network according to the degree, betweenness, and closeness scores by applying the CytoNCA plug-in.

2.1.5 GO and KEGG pathway analysis

For GO enrichment analysis and KEGG pathway analysis, the bioinformatics database Metascape (https://metascape.org/) offers extensive gene and protein bioinformatics [26]. Finally, the key signaling pathways obtained in Metascape with the restrictive criterion $p < 0.01$, were displayed using a bioinformatics online tool (http://www.bioinformatics.com.cn/).

2.1.6 Molecular docking

The protein 3D structures of the putative targets were obtained from the RCSB Protein Data Bank (http://www.pdb.org/) and modified by removing

water and ligands by PyMOL2.4.0 software (https://www.lfd.uci.edu/~gohlke/pythonlibs/). The 3D chemical structural formulae of ligands were retrieved from the PubChem database and translated into PDB files with the help of the OpenBable2.4.1 software (http://openbabel.org/). Molecular docking was performed using AutoDock4.2.6 software (https://autodock.scripps.edu/), whereas the obtained results were visualized with PyMOL2.4.0 software.

2.2 Experimental Validation

2.2.1 Tanshinones combinations preparation

Tanshinone IIA, cryptotanshinone, tanshinone I, and dihydrotanshinone I were purchased from Shanghai Yuanye Bio-Technology Co., Ltd (Shanghai, China). DST1 is a combination of cryptotanshinone and dihydrotanshinone I in a ratio of 5 : 2; DST2 is a combination of tanshinone IIA, cryptotanshinone, tanshinone I and dihydrotanshinone I in a ratio of 6 : 5 : 2 : 2. 1-Methyl-3-nitro-1-nitrosoguanidine (MNNG, purity ⩾ 95%, CAS. No. 70-25-7) was purchased from Shanghai Macklin Biochemical Co., Ltd (Shanghai, China). MNNG was dissolved in DMSO and would be diluted with DMEM (C11965500BT, Gibco, China) to the relevant concentration before experiment.

2.2.2 Cell lines and culture condition

GES-1 cell lines were presented by Professor Huajun Zhao from the School of Pharmaceutical Sciences of Zhejiang Chinese Medical University. Cells were cultivated in a DMEM solution containing 10% FBS (70220-8611, Zhejiang Tianhang Biotechnology Co., Ltd., China), 100 units/mL penicillin, and 100 g/mL streptomycin within a 37 ℃, 5% CO_2 incubator.

2.2.3 Cell viability assay

GES-1 cells in the logarithmic growth phase were collected and planted into 96-well plates with concentration as 8 × 10^3 cells per well. The cells were divided into blank control group and drug treatment groups with different concentrations of DST1 (400, 200, 100, 50, 25, 12.5 μM) and DST2 (400, 200, 100, 50, 25, 12.5 μM), with four parallel wells in each group. Each well received 10 μL of CCK-8 reagent (BS350A, Biosharp, China) after 24 hours of cell culture, and then the cells were incubated for an additional 4 hours. Then the optical density (OD) value of each well was detected by a microplate reader (Power Wave 340, BIO-TEK, America) at 450 nm, the cell viability was calculated according to the formula as follow: cell viability (%) = (OD treatment/OD control) × 100.

MNNG is a classical chemical carcinogen, which is widely used to induce gastric mucosal epithelial cell injury and precancerous lesion models [27]. The effect of MNNG on GES-1 cell viability also was measured by CCK-8 assay. After 24 hours incubation with various MNNG concentrations (5, 1, 0.5, 0.35, 0.25, 0.1 μM), the viability of GES-1 cells was assessed. Aimed to measure the protective effect of tanshinones combination on MNNG-induced CAG, DST1 (200, 100, 50, 10, 2, 0.2, 0.04 μM) and DST2 (50, 25, 12.5, 2.5, 0.5, 0.1, 0.01 μM) were applied to GES-1 cells co-cultured with MNNG (0.35 μM), and after 24 hours treatment, the cell viability in each group was monitored by CCK-8.

2.2.4 Western blotting assay

GES-1 cells in the group that co-culture with MNNG (0.35 μM) was exposed to DST1 (100, 10, 1 μM) and DST2 (25, 2.5, 0.25 μM) for 24 hours. The model group and blank control group were treated with medium simultaneously. The cells from the aforementioned groups were collected and washed with cold PBS twice. They were then suspended in 100 mL of protease inhibitors-containing cell lysate and disrupted on ice for 30 minutes. After centrifugation for 15 minutes at 14,000 rpm and 4 ℃, the supernatant was collected, and the protein

concentration was measured by BCA. 15 μg protein of each group was applied to perform the SDS-PAGE gel electrophoresis, then subsequently transferred to a polyvinylidene fluoride (PVDF) membrane. The membrane was blocked with a TBST solution containing 5% low-fat dried milk for 2 hours, followed an incubation of primary antibodies of GAPDH (1: 5000, R1210-1, HUABIO, China), STAT3 (1: 1000, MB0354, Abmart, China), p-STAT3 (1:1000, T56566F, Abmart, China), EGFR (1: 1000, ET1604-44, HUABIO, China), and Caspase-3 (1: 1000, bs-0081R, Bioss, China), and corresponding rabbit secondary antibodies (RGAR006, Proteintech, China). Then the membranes added with the Omni-ECL TM Enhanced Pico Light Chemiluminescence reagent were placed in a Bio-Rad chemiluminescence imaging system for exposure. The ImageJ v1.53 software (https://imagej.nih.gov/ij/) was used for gray value calculation and quantitative analysis with GAPDH serving as an internal reference.

2.2.5 Immunofluorescence assay

The logarithmic phase GES-1 cells were collected and inoculated onto the slides of cells placed 24-well plates at 2×10^4 per well. After cells attachment, GES-1 cells in the group that co-culture with MNNG (0.35 μM) was exposed to DST1 (100, 10, 1 μM) and DST2 (25, 2.5, 0.25 μM) for 24 hours. The model group and blank control group were treated with medium simultaneously. The cells were fixed for 30 minutes with 4% paraformaldehyde, blocked with QuickBlock ™ Blocking Buffer (P0222, Beyotime Biotechnology, China) for 10 minutes and then incubated with Anti-EGFR Recombinant Rabbit Monoclonal Antibody (Hangzhou Huaan Biotechnology Co., Ltd.) at 4 ℃ overnight. After rinsing with PBS, fluorescein-labeled secondary antibody FITC Goat Anti-Rabbit IgG was added and incubated at room temperature in dark for 1 hour. Finally, after adding anti-fluorescence quencher with DAPI, the slides were photographed under an inverted fluorescence microscope (IX71, OLYMPUS, Japan).

2.2.6 TUNEL apoptosis assay

The logarithmic phase GES-1 cells were collected and cultured on 24-well plates with 2×10^4 cells per well. After cells attachment, GES-1 in co-culture with MNNG (0.35 μM) was exposed to DST1 (100, 1 μM) and DST2 (25, 0.25 μM) for 24 hours. The model group and blank control group were established simultaneously. The cells were fixed for 30 minutes with 4% paraformaldehyde before being treated for 5 minutes at room temperature with PBS containing 0.3% Triton X-100. Subsequently, the sample was given 50 μL of TUNEL detection solution, and it was then incubated for 60 minutes at 37 ℃ without light. Eventually, the slides were viewed under an inverted fluorescence microscope after being sealed with an anti-fluorescence quenching sealing solution. The fluorescence image was converted into 8 bit grayscale image in ImageJ (v1.53) software, and the optical density correction was carried out after black and white inversion. A fixed threshold was applied to all images using ImageJ (v1.53) to distinguish TUNEL-positive signals from background. The Area and Intden values were obtained by software analysis and measurement. Relative fluorescence intensity = TUNEL IntDen/DAPI Area. Semi-quantitative comparison can be made after measuring the average optical density of multiple images by the same method.

2.3 Statistics analysis

The GraphPad Prism software 9.3.0 was applied to perform statistical analysis. The *t*-test was used to examine how the mean values of the two groups differed. The significance level was set at $p < 0.05$. All data were presented in the form of mean ± standard error of mean.

3 Results

3.1 Identification of tanshinones targets for GAC therapy

12 active tanshinones were obtained from the SwissTarget Prediction and TCMSP after deduplication and ADME screening. These compounds are generally abundant and active in *S. miltiorrhiza*. After eliminated the duplicates, 214 targets of tanshinones were determined. Meanwhile, a total of 663 disease targets screened from the GeneCard database were intersected with the aforementioned 214 targets, and 42 common targets were finally identified as the potential targets, as shown in the Venn diagram of Figure 1A.

3.2 Compound-Target network development and PPI analysis

The compound-target network is shown in Figure 1B. According to the compound-target network of tanshinone for GAC therapy (Figure 1B), it was found that the degree value of cryptotanshinone was the highest, followed by dihydrotanshinone I. These two kinds of tanshinones may exhibited important effects in the treatment. Figure 1C demonstrates the PPI relationship (39 nodes and 230 edges). The darker colors and larger sizes signify a greater degree. According to Figure 1D, the seven hub targets from the PPI network that had the greatest degree values were ranked by degree as CASP3, EGFR, STAT3, PTGS2, MMP2, ERBB2, and PPARG.

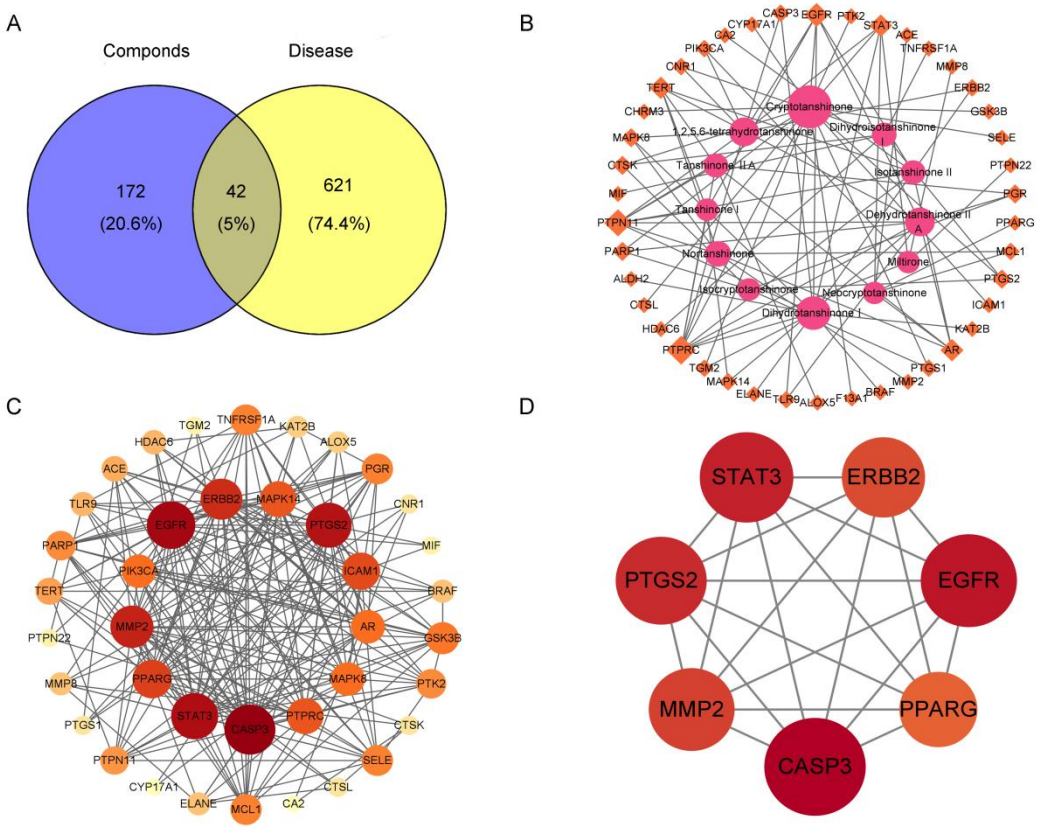

Figure 1 Results of network pharmacology analysis. (A) Venn diagram of drug targets and disease proteins. (B) compound-target network construction. Pink circles represent compounds; Orange diamond represent targets. (C) PPI network of candidate targets of tanshinones against CAG. The larger sizes and darker colors indicate a higher degree. (D) Map of the central network.

3.3 GO enrichment and KEGG pathway analysis

Firstly, 656 GO keywords were enriched in the biological enrichment analysis of 42 common targets (p-value $\leqslant$ 0.05). The 43 functional clusters associated with cell component (CC) were mostly consist of membrane rafts, vesicle lumens, and

extracellular matrix that contains collagen (Figure 2A). A total of 54 functional clusters related to the molecular functions (MF) were displayed, and kinase binding, transcription factor binding and protein phosphatase binding were inclusive (Figure 2B). The findings elucidated that there were 559 functional clusters associated with the biological processes (BP), such as cellular response to organonitrogen compound and positive regulation of protein phosphorylation (Figure 2C). Meanwhile, the top 15 signaling pathways of common targets, including proteoglycans in cancer, lipid and atherosclerosis, fluid shear stress and atherosclerosis, apoptosis, human cytomegalovirus infection, were shown in Figure 2D. According to KEGG analysis, tanshinones were thought to have an effect on the CAG therapy via the aforementioned numerous pathways.

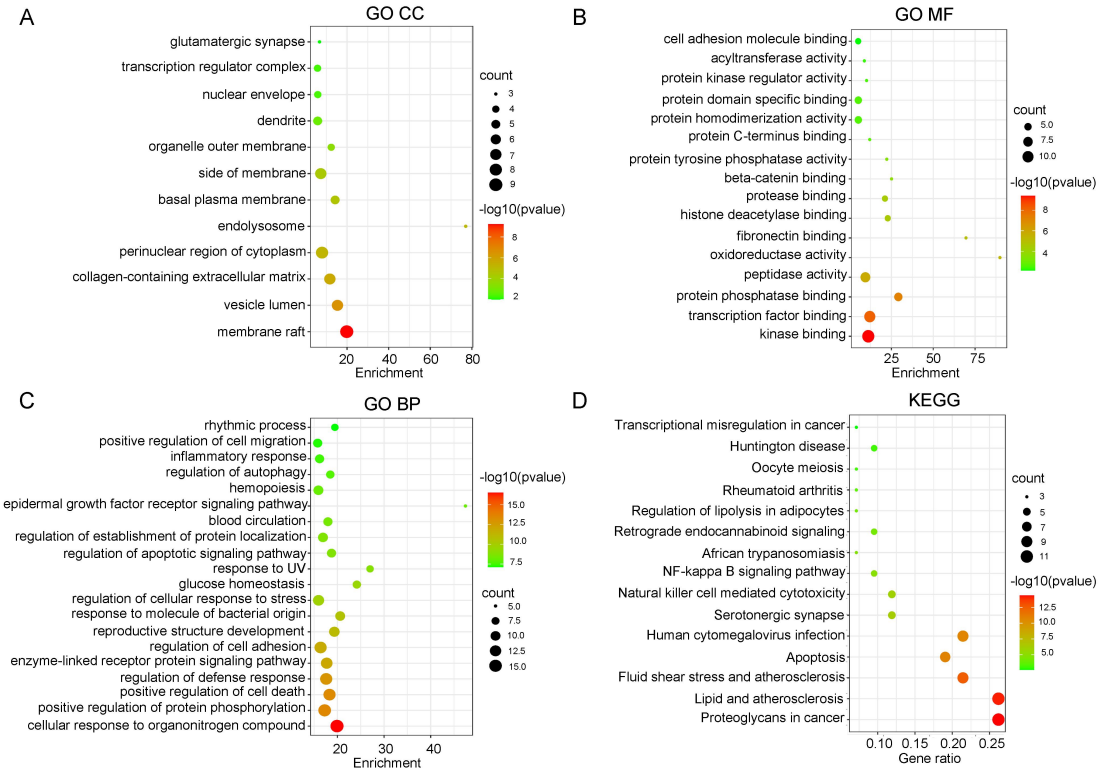

Figure 2 GO and KEGG enrichment of screened targets. (A) GO CC enrichment analysis. (B) GO MF enrichment analysis. (C) GO BP enrichment analysis. (D) KEGG pathway enrichment of the candidate targets of tanshinones in the treatment of CAG. The size of the circles represents the number of genes and the color represents the *p* value.

3.4 Molecular docking

For the sake of further exploration of the interaction between the active ingredients and key targets of tanshinones, the four active ingredient of cryptotanshinone, tanshinone IIA, dihydrotanshinone I, and tanshinone I, and the top two key targets (EGFR, STAT3) of the degree value were selected and verified by molecular docking. The binding energy less than zero is a necessary condition for the spontaneous binding of the target gene to the active component, and when it is less than -5.0 kcal/mol, the binding activity is considered to be stronger. The results suggested that tanshinones might influence EGFR and STAT3 to prevent CAG. In all binding findings, it was discovered that cryptotanshinone and STAT3 displayed the highest binding affinities (Table 1). Figure 3 represented molecular docking visually and showed how the chemicals and targets interacted. Cryptotanshinone makes hydrogen bonds (yellow dotted line) with APS-369 from EGFR and STAT3.

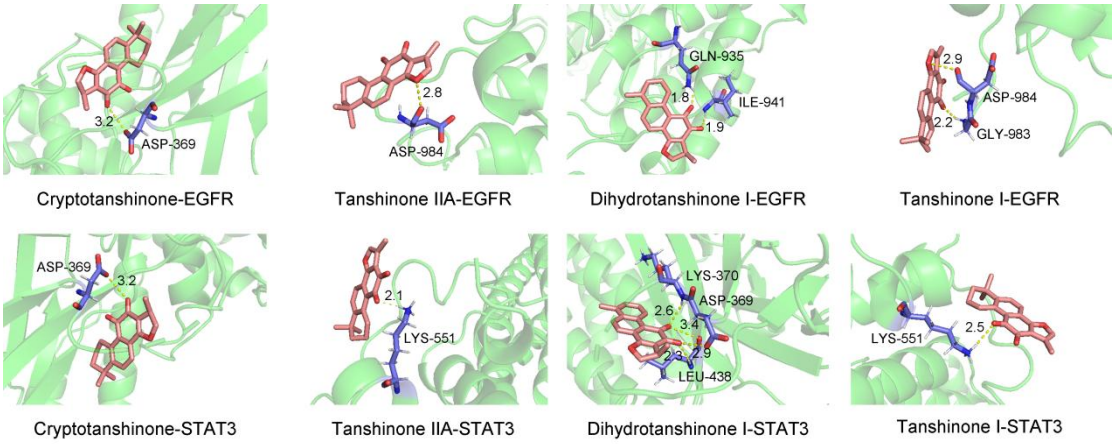

Figure 3 Visualization of molecular docking. The pink molecular structure represents the drug molecule, and the green is the receptor protein. The blue structures represent the amino acid residues of the receptor binding to tanshinone. The yellow dotted lines represent the hydrogen bonds; the number represents the hydrogen bond length.

Table 1 Docking results of STAT3 and EGFR with the active compounds.

Target	Compound	Binding energy/(kcal·mol^{-1})
EGFR	Cryptotanshinone	-4.91
EGFR	tanshinone IIA	-4.71
EGFR	dihydrotanshinone I	-4.88
EGFR	tanshinone I	-4.79
STAT3	Cryptotanshinone	-5.44
STAT3	tanshinone IIA	-4.79
STAT3	dihydrotanshinone I	-5.41
STAT3	tanshinone I	-4.62

3.5 Effect of tanshinones combination on GES-1 cell's viability

To evaluate the appropriate concentrations of MNNG, DST1 and DST2, the CCK-8 kit was used to assess the GES-1 cells viability. The results indicated that when the concentration of DST1 was less than or equal to 200μM and the concentration of DST2 was less than or equal to 50 μM, they had insignificant influence on the cell viability (Figure 4A-B). MNNG treatment significantly reduced GES-1 cell viability in a dose-dependent manner. At 0.35 μ M, MNNG decreased cell viability to 68.5 ± 3.2% compared to the control group ($p < 0.01$), indicating sublethal damage suitable for modeling chronic atrophic gastritis (Figure 4C).The threshold concentration of MNNG with cell viability greater than 60% was selected, and 0.35 μM was determined as the most appropriate concentration for modeling according to the results (Figure 4C). Furthermore, to explore the effects of the tanshinones combinations, various concentrations of DST1 and DST2 were applied to GES-1 that was co-cultured with MNNG on the basis of the aforementioned findings. Subsequent experimental results showed that DST1 at various concentrations had inconspicuous protective effects on GES-1, and the effect of 10 μM was slightly better compared with other concentrations (Figure 4D). But for DST2, it reflected an obvious concentration effect

trend, and 2.5 μM displayed notable protective effects on GES-1 (Figure 4E).

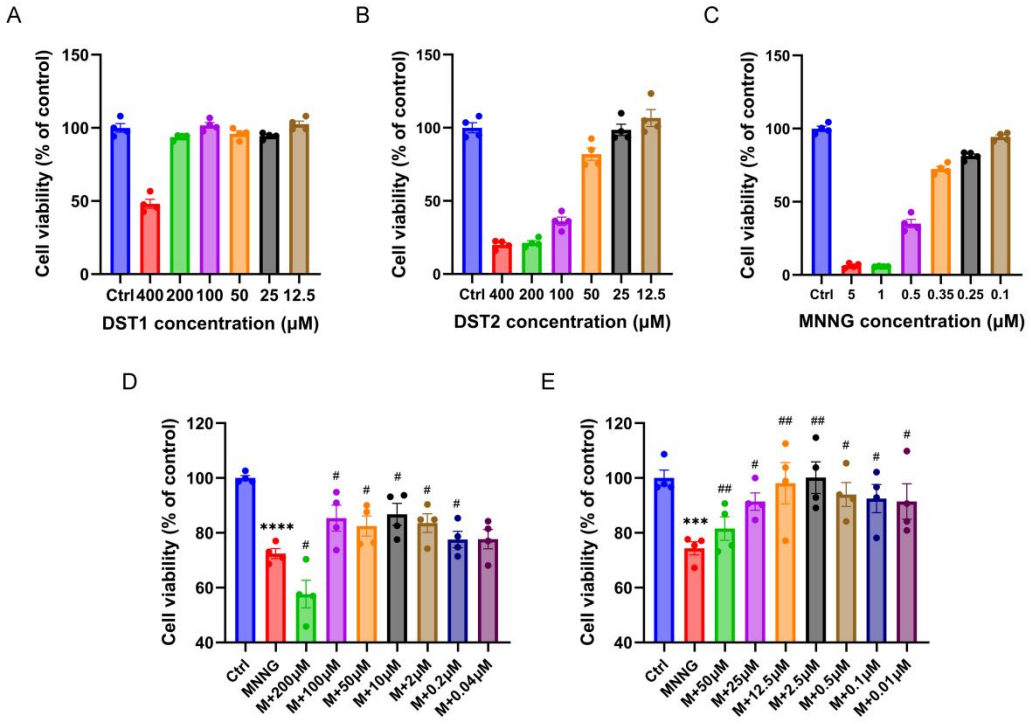

Figure 4 Effects of tanshinones combination and MNNG on GES-1 cells *in vitro*. Effects of DST1 (A), DST2 (B), and MNNG (C) with different concentrations on the viability of GES-1 after treated for 24 h. Effects of DST1 (D) and DST2 (E) with different concentrations on the viability of GES-1 cells co-cultured with 0.35 μM MNNG. Data were shown as mean ± SEM. N = 4. **** $p < 0.0001$ versus control group; *** $p < 0.001$ versus control group. $^{\#\#}p < 0.01$ versus MNNG group; $^{\#}p < 0.05$ versus MNNG group. Ctrl: Control; M: MNNG.

3.6 Inhibition of EGFR-STAT3 pathway by tanshinones combinations

Western blot analysis revealed that, in comparison to the control group, MNNG treatment significantly increased the expression of EGFR, STAT3, and Caspase-3 ($p < 0.05$) (Figure 5B-D). However, the DST intervention dramatically reduced the protein expression of EGFR, STAT3, and Caspase-3 ($p < 0.05$, $p < 0.01$, $p < 0.001$) (Figure 5B-D). And DST1 and DST2 were found to inhibit the expression of phosphorylated-STAT3 (Figure 5E). However, DST1 and DST2 subtlely increase the values of p-STAT3/STAT3 (Figure 5F). Through the immunofluorescence detection of EGFR, it was further confirmed that EGFR was inhibited by tanshinones combinations (Figure 6A-B).

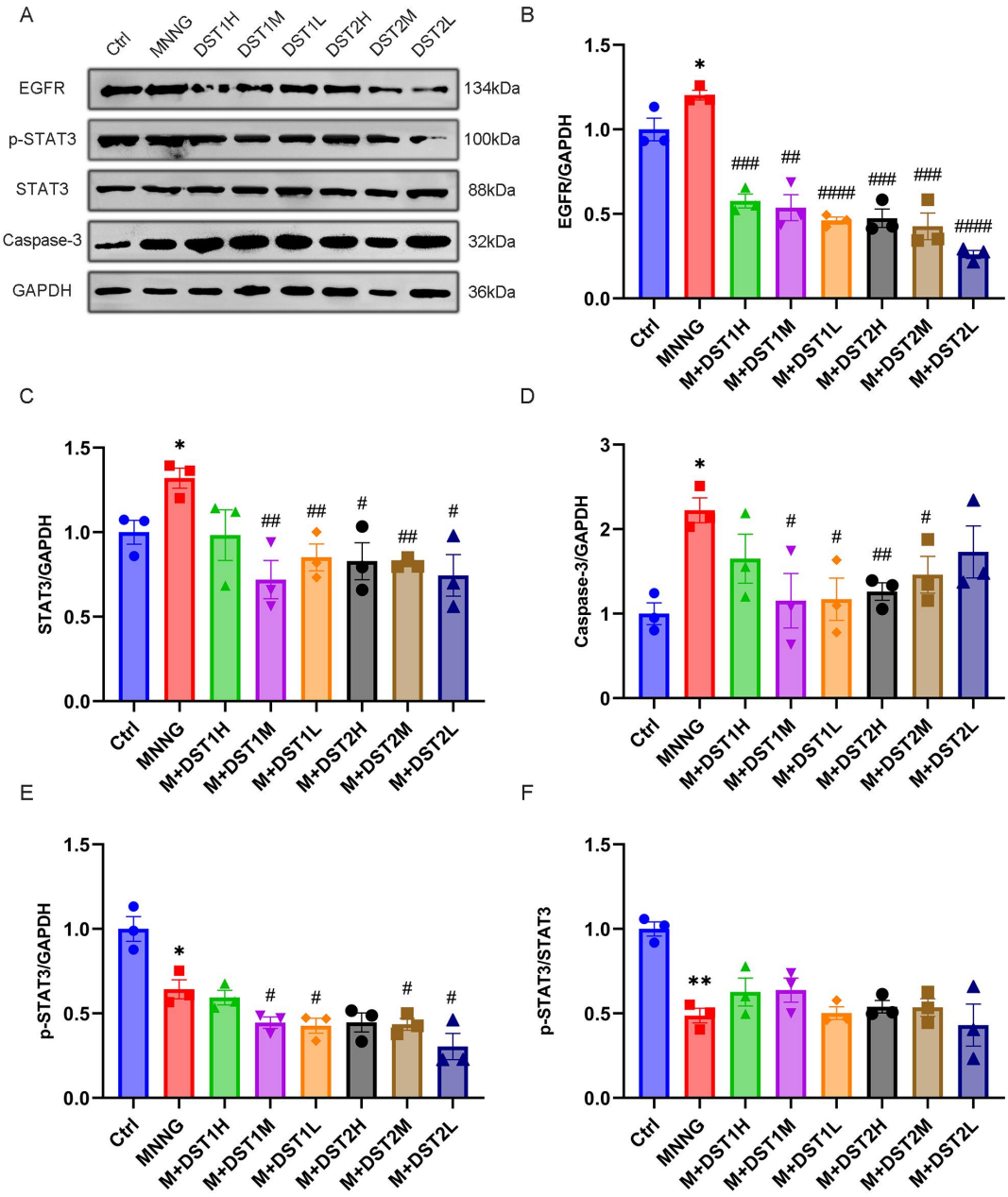

Figure 5 Effect of tanshinones combinations DST1 and DST2 in expression of EGFR-STAT3 signaling pathway-related proteins. (A) Western blot images of EGFR, p-STAT3, STAT3, Caspase-3, and GAPDH. (B-F) Relative expression of EGFR (B), STAT3 (C), Caspase-3 (D), p-STAT3 (E), and p-STAT3/STAT3 (F) protein in GES-1 cells (N = 3). Data were shown as mean ± SEM. * $p < 0.05$, ** $p < 0.01$ versus control group; $^{\#}p < 0.05$, $^{\#\#}p < 0.01$, $^{\#\#\#}p < 0.001$, and $^{\#\#\#\#}p < 0.0001$ versus MNNG group. Ctrl, Control; M, MNNG; DST1H, DST1 high dose group (100 μM); DST1M, DST1 medium dose group (10 μM); DST1L, DST1 low dose group (1 μM); DST2H, DST2 high dose group (25 μM); DST2M, DST2 medium dose group (2.5 μM); DST2L, DST2 low dose group (0.25 μM).

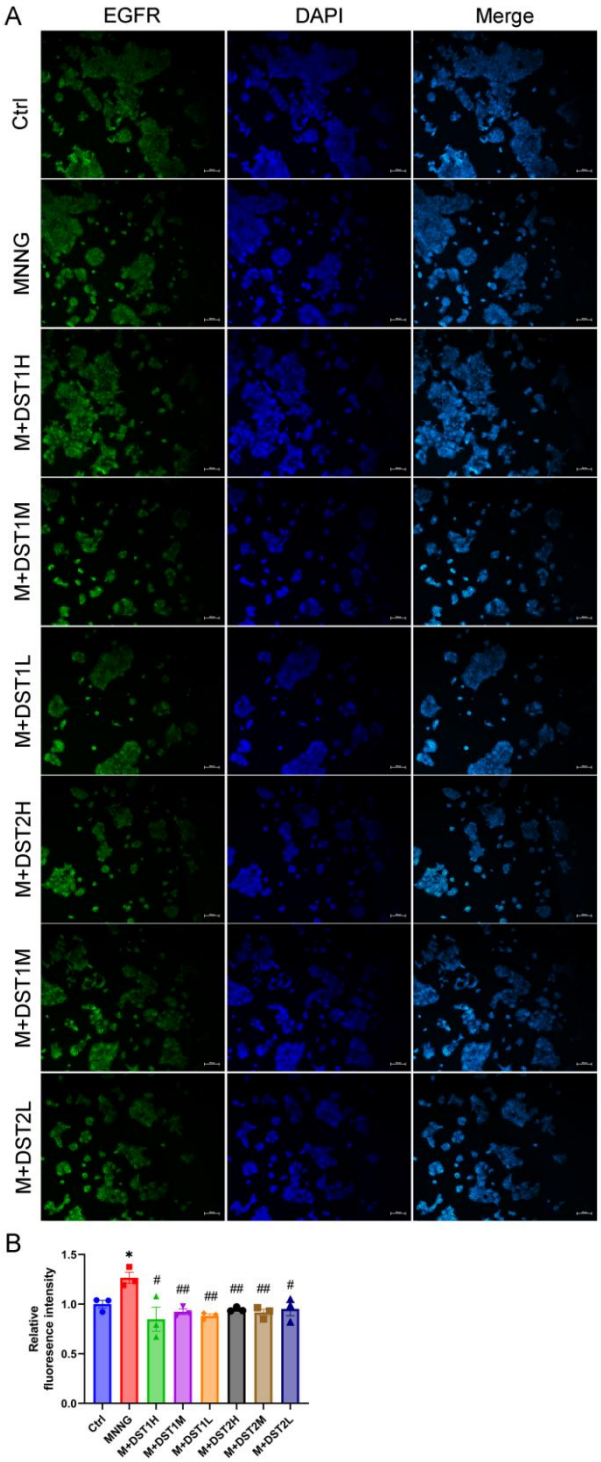

Figure 6 Immunofluorescence of EGFR. (A) Immunofluorescence images of EGFR (scale bar = 100 μm, magnification, ×100). EGFR positive staining cells showed green (N = 3). (B) Relative fluorescence intensity of EGFR. Data were shown as mean ± SEM. * $p < 0.05$ versus control group; $^{\#}p < 0.05$, $^{\#\#}p < 0.01$ versus MNNG group. Ctrl, Control; M, MNNG; DST1H, DST1 high dose group (100 μM); DST1M, DST1 medium dose group (10 μM); DST1L, DST1 low dose group (1 μM); DST2H, DST2 high dose group (25 μM); DST2M, DST2 medium dose group (2.5 μM); DST2L, DST2 low dose group (0.25 μM).

3.7 Effect of tanshinones combinations on cell apoptosis

In view of the Western blot results, we selected low and high concentrations of DST1/2 as experimental

groups to examine the impact of tanshinones combinations on cell apoptosis by TUNEL analysis. After TUNEL positive cells were photographed by fluorescence microscope, semi-quantitative analysis was performed using Image J software (version 1.53). A fixed threshold was set to distinguish positive signals, and the proportion of positive cells per field and the average fluorescence intensity were calculated (the number of cells was corrected based on DAPI staining). By quantifying TUNEL-positive nuclei and the mean fluorescence intensity, the ratio of apoptosis in model group was found to be obviously higher than that of the control group, DST1H, DST1L and DST2H groups ($p < 0.01$, $p < 0.05$, $p < 0.001$) (Figure 7A-B). The findings indicated that DST1/2 could concentration-dependently inhibit MNNG-induced GES-1 cell apoptosis.

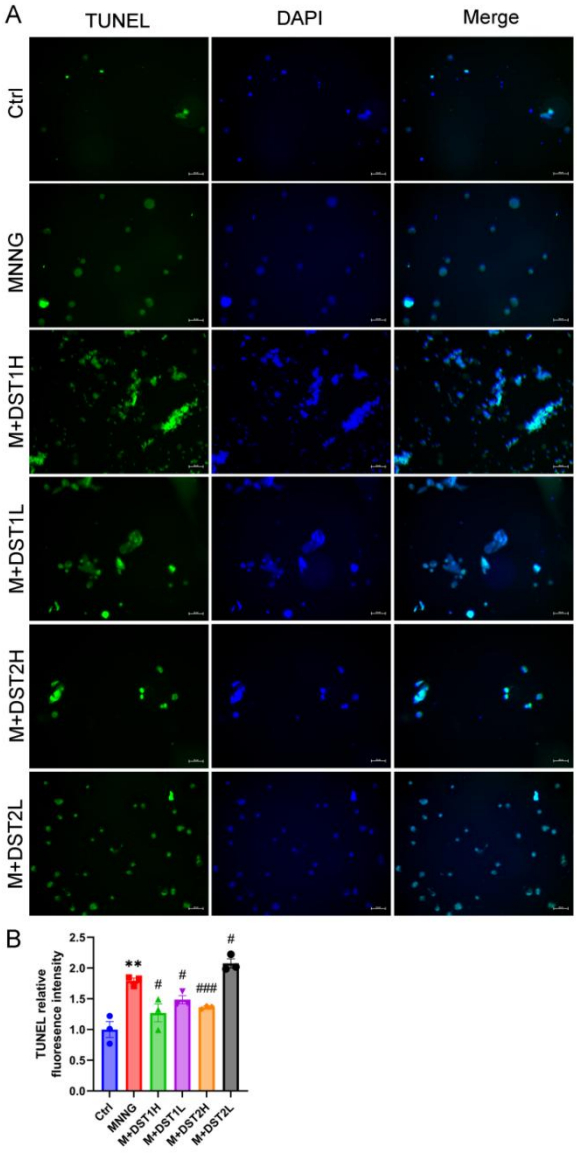

Figure 7 Effect of tanshinones combinations on cell apoptosis. (A) Representative images of TUNEL assay of tanshinones combinations DST1 and DST2 in MNNG-induced GES-1 cells (scale bar = 50 μm, magnification, × 200). TUNEL positive staining cells showed green (N = 3). (B) TUNEL relative fluorescence intensity. Data were shown as mean ± SEM. ** $p < 0.01$ versus control group; $^{\#}p < 0.05$, $^{\#\#}p < 0.01$, $^{\#\#\#}p < 0.001$ versus MNNG group. Ctrl, Control; M, MNNG; DST1H, DST1 high dose group (100 μM); DST1L, DST1 low dose group (1 μM); DST2H, DST2 high dose group (25 μM); DST2L, DST2 low dose group (0.25 μM).

4 Discussion

As a common precancerous condition, CAG shows a remarkable correlation with gastric cancer. An annual incidence rate of 1.36% person/year for gastric neoplastic lesions has been reported in CAG patients [28]. Hence, effective intervention in CAG may provide an available strategy for the prevention of gastric cancer.

The occurrence and development of tumors are known to be influenced by the multiple factors, and the same is true of CAG. Drugs targeting one pathway or a single target actually show good efficacy in the early stages of treatment, but then often lead to a significant decline in efficacy as tumor cells evade drug treatment through other pathways [29]. Great concern has been aroused that the combination of drugs acting on multiple targets at the same time can produce more effective and longer-lasting therapeutic effects, while reducing the dosage and side effects. The efficacy of Moluodan combined with rabeprazole in the treatment of chronic gastritis is significantly manifested as promoting gastric mucosal repair, reducing inflammatory damage, and no significant increase in adverse reactions, with high safety [30]. Through evaluating the feasibility and efficacy of combined chemotherapy, it was clear that the combination therapy could greatly alleviate the clinical symptoms experienced by gastric cancer patients, providing data support for the further application of combination therapy in cancer treatment [31]. Triptolide enhanced the cytotoxic effect of cisplatin on gastric cancer SC-M1 cells through mitochondrial-mediated apoptosis pathway, suggesting that the combination therapy improved the synergistic anticancer activity [32]. Moreover, the problems of low efficacy, patient intolerance and serious adverse reactions of traditional chemotherapy drugs remained a challenge in most gastric cancer and CAG patients, but combination therapy made it possible to alleviate these problems, providing potential therapeutic regimen for patients with CAG and gastric cancer [33].

Network pharmacology has created a new model of drug research with multi-target, synergistic, and superimposed effects, which has potential application value in the study of pathogenesis and therapeutic targets of complex diseases. The most important thing of TCM treatment theory is to prevent and treat diseases from the overall concept, which is congruent with the network pharmacology concept of multi-component, multi-target, and multi-channel prevention and treatment of diseases [34]. We selected the two compounds (cryptotanshinone and dihydrotanshinone I) with the highest degree values and lowest binding energy to EGFR and STAT3 on the basis of 12 active ingredients of tanshinones by network pharmacology and molecular docking analysis. We formed this two compounds into the first tanshinone composition named DST1. Furthermore, our previous reports also demonstrated that tanshinone I and tanshinone IIA-rich diterpenoids isolated from *Salvia miltiorrhiza* exhibited tumour-suppressive effects in multiple human tumor cell lines *in vitro* [18]. Therefore, we selected cryptotanshinone, tanshinone IIA, dihydrotanshinone I, and tanshinone I, which have been proved to have anti-tumor activity, to form the second tanshinone composition named DST2. The assay for cell viability demonstrated that the minimum concentration of DST2 was lower than that of DST1 when MNNG-induced GES-1 cell viability was the same. Moreover, DST2 can exert a better protective effect on cells apoptosis, more in line with the clinical low-cost, efficient principle. We focused on the apoptosis pathway and EGFR-STAT3 signaling pathway in accordance with the network pharmacology analysis of the pathways and targets of tanshinones for CAG therapy. EGFR-STAT3 signaling pathway is one of several pathways triggered by activated EGFR. STAT3 directly binds to EGFR through the SH2 domain and is

activated by EGFR, which results in homodimerization or heterodimerization of STAT3 and then contributes to its nuclear localization and DNA binding [35]. EGFR/STAT3 signaling pathway is up-regulated in tumors which regulates cell proliferation and apoptosis by affecting a variety of downstream effector molecules through a complicated network, thus inducing tumorigenesis [36].

This study revealed for the first time that tanshinone combination (DST1/DST2) reduces MNNG-induced GES-1 cell apoptosis by inhibiting EGFR-STAT3 signaling pathway, providing a new idea for CAG treatment. Although the role of EGFR-STAT3 pathway in gastric cancer has been reported [37], its role in CAG remains unclear. Our results showed that the expression of EGFR and STAT3 was significantly up-regulated in MNNG-induced CAG model, and tanshinone combination could reverse this phenomenon, suggesting that this pathway may promote precancerous lesions by regulating apoptosis and chronic inflammation in CAG progression. Although there have been few studies highlighting the activation of EGFR/STAT3 signaling pathway in CAG, both EGFR and STAT3 have been implicated in the advancement of CAG. EGFR is a transmembrane tyrosine kinase that regulates various biological processes, including proliferation, apoptosis, metabolism, migration, and differentiation [38]. EGFR is activated by ligand-mediated dimerization and autophosphorylation, thereby activating downstream signal transduction factors [38]. Previous research on EGFR found it to be strongly expressed in various cancers including colon, breast, and gastric cancers [39]. Moreover, Wei-Wei-Kang-Granule was thought to ameliorate chronic atrophic gastritis through reducing the levels of NF-κB and EGFR [40]. Through the inhibition of MMP-10 via the blockage of ADAM17/EGFR signaling, palmatine displayed considerable protective effects against helicobacter pylori-induced CAG [41]. The STAT3 is a crucial transcription factor that mediates cytokine and growth factor responses [42]. Sustained STAT3 activation considerably promotes chronic inflammation, thereby increasing the possibility of cell carcinogenesis [43]. The continuous activation of STAT3 was closely related to the proliferation and inflammation of the helicobacter-associated gastric epithelium and exhibited as a key factor in promoting gastric carcinogenesis [44]. Above all, previous research has elucidated the critical involvement of EGFR and STAT3 in the pathogenesis and treatment of CAG. Therefore, tanshinone may interfere with the EGFR-STAT3 axis through multiple targets and block the key steps in the transformation of CAG to gastric cancer.

In order to explore the underlying mechanism of tanshinones combinations on protecting cells under CAG condition and preventing the further carcinogenesis, the expression of proteins connected to the EGFR-STAT3 signaling pathway was examined by Western blot. Tanshinones can reduce the levels of EGFR, STAT3, and Caspase-3. The experimental results further verified the hypothesis that EGFR and STAT3 are highly expressed in CAG cells induced by MNNG and are positively correlated. As an important effector of apoptosis, Caspase-3 can be found abnormally high expression in MNNG-induced chronic atrophic gastritis cells by western blot. The STAT3 pathway has been shown to inhibit the caspase cascade and block the initiation of apoptosis by activating apoptosis inhibitors in tumor cells [45]. Therfore, we speculated that tanshinones can inhibit apoptosis through hindering the EGFR-STAT3 signaling pathway, consequently preventing CAG cell transition into cancer cells.

Apoptosis is one of the physiological processes of cells, which can not only eliminate unnecessary or abnormal cells, but also contribute greatly to the prevention of tumorigenesis [46]. Precancerous lesions have been found to exhibit a higher rate of apoptosis than normal

tissues and gastric cancer [47]. The TUNEL assay results from our investigation demonstrated that the high concentration of tanshinones combination could effectively inhibit apoptosis of MNNG-induced GES-1 cells, suggesting that tanshinones have the effect to block the progress of CAG to gastic cancer. However, DST2L (0.25 μ M) showed a marginal increase in TUNEL fluorescence intensity compared to the MNNG group, this effect suggests that higher concentrations of DST2 are required for robust anti-apoptotic activity.

In general, the results of this study demonstrated that tanshinones combinations may suppress the gastric epithelial mucosal cells apoptosis via inhibiting EGFR/STAT3 signaling pathway. Although this study preliminarily revealed the potential of tanshinone to inhibit EGFR-STAT3 pathway through *in vitro* experiments, its specific mechanism in CAG treatment still needs to be further verified. Firstly, it is necessary to verify the *in vivo* efficacy and pathway inhibition of tanshinone in animal models (such as MNNG-induced CAG model in mice). Secondly, by combining EGFR inhibitors (such as gefitinib) or STAT3 activators (such as IL-6), it is clear whether tanshinone specifically relies on this pathway to play a role. In addition, the correlation between the level of EGFR/STAT3 phosphorylation in clinical sample analysis (such as gastric mucosa of CAG patients) and the efficacy of tanshinone will enhance the transformation value of the research conclusions. Moreover, although chronic inflammation is a hallmark of CAG, this study primarily focused on the EGFR-STAT3-apoptosis axis. Future work should integrate cytokine profiling (e.g., IL-6, TNF- α) to comprehensively evaluate tanshinones ' anti-inflammatory effects in CAG.

Despite the above limitations, the low toxicity (CCK-8 showed no significant cell inhibition at ⩽ 50 μM) and multi-target characteristics of tanshinone combination provide advantages for its clinical transformation. Future studies can design long-term animal intervention experiments to evaluate the effect of tanshinone on CAG pathological reversal, such as gastric gland atrophy, intestinal metaplasia, and explore its synergistic effect with existing therapies including proton pump inhibitors. In addition, based on the fat-soluble characteristics of tanshinone, the development of delivery systems targeting gastric mucosa such as nano-preparations may further enhance its efficacy.

5 Conclusion

Tanshinones combination exhibits a positive impact on the anti-CAG response elicited by MNNG *in vitro*, and this function is correlated with the suppression of EGFR-STAT3 signaling pathway and cell apoptosis.

Abbreviations

ADME: Absorption, Distribution, Metabolism, Excretion; CAG: Chronic Atrophic Gastritis; CASP3: Caspase-3; CCK-8: Cell Counting Kit-8; DAPI: 4', 6-Diamidino-2-Phenylindole; DL: Drug-likeness; DMEM: Dulbecco ' s Modified Eagle Medium; EGFR: Epidermal Growth Factor Receptor; ERBB2: Erb-B2 Receptor Tyrosine Kinase 2; FBS: Fetal Bovine Serum; GC: Gastric Cancer; GO: Gene Ontology; Hp: Helicobacter pylori; HRP: Horseradish Peroxidase; KEGG: Kyoto Encyclopedia of Genes and Genomes; MMP2: Matrix Metalloproteinase 2; MNNG: N-methyl-N'-nitro-N-nitrosoguanidine; NF- κ B: Nuclear Factor Kappa B; OB: Oral Bioavailability; PPARG: Peroxisome Proliferator Activated Receptor Gamma; PPI: Protein-Protein Interaction; PTGS2: Prostaglandin-Endoperoxide Synthase 2; PVDF: Polyvinylidene Fluoride; SDS-PAGE: Sodium Dodecyl Sulfate-Polyacrylamide Gel Electrophoresis; SEM: Standard Error of Mean; STAT3: Signal Transducer and Activator of Transcription 3; TBST: Tris-Buffered Saline with Tween 20; TCM: Traditional Chinese Medicine; TCMSP: Traditional Chinese Medicine Systems Pharmacology Database and Analysis Platform; TUNEL: Terminal deoxynucleotidyl transferase dUTP

nick end labeling.

Acknowledgements

We acknowledge TCMSP and GeneCards databases for providing their platforms as well as contributors for uploading their meaningful datasets.

Conflicts of Interest

All authors declare that they have no conflicts of interest.

Author Contributions

Y.W.: Project design, Project administration, Writing - original draft; H.H.: Project design, Visualization; L.H.: Methodology; Z.L.: Conceptualization, Funding acquisition, Writing - review & editing.

Ethics Approval and Consent to Participate

No ethical approval was required for this review article.

Funding

This work was supported by the State Key Program of the National Natural Science Foundation of China (No. 82030119 to ZGJ); the Zhejiang Xinmiao Talents Program (No.752213A13019); the Zhejiang Traditional Chinese Medicine Science and Technology Plan (No. 2021ZB214).

Availability of Data and Materials

Data supporting this study are included within the article or openly available from various databases mentioned in 2.1.

Supplementary Materials

Not applicable.

References

[1] Rodriguez-Castro KI, Franceschi M, Noto A, et al. Clinical manifestations of chronic atrophic gastritis. *Acta bio-medica: Atenei Parmensis* 2018; 89(8-S): 88-92.

[2] Annibale B, Esposito G, Lahner E. A current clinical overview of atrophic gastritis. *Expert Review of Gastroenterology & Hepatology* 2020; 14(2): 93-102.

[3] Correa P. Helicobacter pylori and gastric carcinogenesis. *American Journal of Surgical Pathology* 1995; 19 Suppl 1: S37-43.

[4] Lahner E, Carabotti M, Annibale B. Treatment of Helicobacter pylori infection in atrophic gastritis. *World Journal of Gastroenterology* 2018; 24(22): 2373-2380.

[5] Fang WJ, Zhang XY, Yang B, et al. Chinese Herbal Decoction as a Complementary Therapy for Atrophic Gastritis: A Systematic Review and Meta-Analysis. *African Journal of Traditional, Complementary, and Alternative Medicines: AJTCAM* 2017; 14(4): 297-319.

[6] Su CY, Ming QL, Rahman K, et al. Salvia miltiorrhiza: Traditional medicinal uses, chemistry, and pharmacology. *Chinese Journal of Natural Medicines* 2015; 13(3): 163-182.

[7] Wang X, Yang Y, Liu X, et al. Pharmacological properties of tanshinones, the natural products from Salvia miltiorrhiza. *Advances in Pharmacology (San Diego, Calif.)* 2020; 87: 43-70.

[8] Xia M, Wu Y, Zhu H, Duan W. Tanshinone I induces ferroptosis in gastric cancer cells via the KDM4D/p53 pathway. *Human & Experimental Toxicology* 2023; 42: 9603271231216963.

[9] Luo N, Zhang K, Li X, et al. Tanshinone IIA destabilizes SLC7A11 by regulating PIAS4-mediated SUMOylation of SLC7A11 through KDM1A, and promotes ferroptosis in breast cancer. *Journal of Advanced Research* 2025; 69: 313-327.

[10] Qian J, Cao Y, Zhang J, et al. Tanshinone IIA induces autophagy in colon cancer cells through MEK/ERK/mTOR pathway. *Translational Cancer Research* 2020; 9(11): 6919-6928.

[11] Lou ZH, Xia RM, Li XJ, et al. Anti-lung cancer mechanisms of diterpenoid tanshinone via endoplasmic reticulum stress-mediated apoptosis signal pathway. *China Journal of Chinese Materia Medica* 2018; 43(24): 4900-4907.

[12] Cui S, Chen S, Wu Q, et al. A network pharmacology approach to investigate the anti-inflammatory mechanism of effective ingredients from Salvia miltiorrhiza. *International Immunopharmacology* 2020; 81: 106040.

[13] Liu X, He H, Huang T, et al. Tanshinone IIA Protects against Dextran Sulfate Sodium- (DSS-) Induced Colitis in Mice by Modulation of Neutrophil Infiltration and Activation. *Oxidative Medicine and Cellular Longevity* 2016; 2016:

7916763.

[14] Yu JR, Liu YY, Gao YY, et al. Diterpenoid tanshinones inhibit gastric cancer angiogenesis through the PI3K/Akt/mTOR signaling pathway. *Journal of Ethnopharmacology* 2024; 324: 117791.

[15] Guan Z, Chen J, Li X, et al. Tanshinone IIA induces ferroptosis in gastric cancer cells through p53-mediated SLC7A11 down-regulation. *Bioscience Reports* 2020; 40(8): BSR20201807.

[16] Gao H, Huang L, Ding F, et al. Simultaneous purification of dihydrotanshinone, tanshinone I, cryptotanshinone, and tanshinone IIA from Salvia miltiorrhiza and their anti-inflammatory activities investigation. *Scientific Reports* 2018; 8(1): 8460.

[17] Liu L, Gao H, Wen T, et al. Tanshinone IIA attenuates AOM/DSS-induced colorectal tumorigenesis in mice via inhibition of intestinal inflammation. *Pharmaceutical Biology* 2021; 59(1): 89-96.

[18] Shen L, Lou Z, Zhang G, et al. Diterpenoid Tanshinones, the extract from Danshen (Radix Salviae Miltiorrhizae) induced apoptosis in nine human cancer cell lines. *Journal of Traditional Chinese Medicine* 2016; 36(4): 514-521.

[19] Lou ZH, Xia RM, Li XJ, et al. Anti-lung cancer mechanisms of diterpenoid tanshinone via endoplasmic reticulum stress-mediated apoptosis signal pathway. *Zhongguo Zhong Yao Za Zhi* 2018; 43(24): 4900-4907.

[20] Zhang R, Zhu X, Bai H, et al. Network Pharmacology Databases for Traditional Chinese Medicine: Review and Assessment. *Frontiers in Pharmacology* 2019; 10: 123.

[21] Li S, Zhang B. Traditional Chinese medicine network pharmacology: theory, methodology and application. Chinese Journal of Natural Medicines 2013; 11(2): 110-120.

[22] Guo B, Zhao C, Zhang C, et al. Elucidation of the anti-inflammatory mechanism of Er Miao San by integrative approach of network pharmacology and experimental verification. *Pharmacological Research* 2022; 175: 106000.

[23] Guo H, Zeng H, Fu C, et al. Identification of Sitogluside as a Potential Skin-Pigmentation-Reducing Agent through Network Pharmacology. *Oxidative Medicine and Cellular Longevity* 2021; 2021: 4883398.

[24] Wen JX, Tong YL, Ma X, et al. Therapeutic effects and potential mechanism of dehydroevodiamine on N-methyl-N'-nitro-N-nitrosoguanidine-induced chronic atrophic gastritis. *Phytomedicine* 2021; 91: 153619.

[25] Ru J, Li P, Wang J, et al. TCMSP: a database of systems pharmacology for drug discovery from herbal medicines. *Journal of Cheminformatics* 2014; 6: 13.

[26] Zhou Y, Zhou B, Pache L, et al. Metascape provides a biologist-oriented resource for the analysis of systems-level datasets. *Nature Communications* 2019; 10(1): 1523.

[27] Aoyagi K, Kohfuji K, Yano S, et al. Morphological change in the MNNG-treated rat gastric mucosa. *The Kurume Medical Journal* 2000; 47(1): 31-36.

[28] Lahner E, Esposito G, Pilozzi E, et al. Occurrence of gastric cancer and carcinoids in atrophic gastritis during prospective long-term follow up. Scandinavian Journal of Gastroenterology 2015; 50(7): 856-865.

[29] Asano T. Drug Resistance in Cancer Therapy and the Role of Epigenetics. *Journal of Nippon Medical School* 2020; 87(5): 244-251.

[30] Ma S, Li Y, Guo R, et al. The Efficacy of Morodan in Combination with Rabeprazole for the Treatment of Chronic Gastritis and its Impact on Gastric Mucosal Repair. *Alternative Therapies in Health and Medicine* 2023; 29(6): 306-310.

[31] Shinkai M, Imano M, Hiraki Y, et al. Combination Chemotherapy Including Intraperitoneal (IP) Administration of Paclitaxel (PTX) followed by PTX, CDDP and S-1 Triplet Chemotherapy for CY1P0 Gastric Cancer. *Gan to kagaku Ryoho. Cancer & Chemotherapy* 2017; 44(12): 1355-1357.

[32] Li CJ, Chu CY, Huang LH, et al. Synergistic anticancer activity of triptolide combined with cisplatin enhances apoptosis in gastric cancer in vitro and in vivo. *Cancer Letters* 2012; 319(2): 203-213.

[33] He X, Zhang T, Wu L, et al. The effect of trifluridine/tipiracil for patients with heavily pretreated metastatic gastric cancer: A protocol for systematic review and meta-analysis. *Medicine (Baltimore)* 2021; 100(2): e24110.

[34] Zhou Z, Chen B, Chen S, et al. Applications of Network Pharmacology in Traditional Chinese Medicine Research. *Evidence-Based Complementary and Alternative Medicine: eCAM* 2020; 2020: 1646905.

[35] Quesnelle KM, Boehm AL, Grandis JR. STAT-mediated EGFR signaling in cancer. *Journal of Cellular Biochemistry* 2007; 102(2): 311-319.

[36] Wu M, Zhang P. EGFR-mediated autophagy in tumourigenesis and therapeutic resistance. *Cancer Letter* 2020; 469: 207-216.

[37] Li SY, Hou LZ, Gao YX, et al. FIP-nha, a fungal immunomodulatory protein from Nectria haematococca,

induces apoptosis and autophagy in human gastric cancer cells via blocking the EGFR-mediated STAT3/Akt signaling pathway. *Food Chemistry* 2022; 4: 100091.

[38] Wee P, Wang Z. Epidermal Growth Factor Receptor Cell Proliferation Signaling Pathways. *Cancers (Basel)* 2017; 9(5): 52.

[39] Rajaram P, Chandra P, Ticku S, et al. Epidermal growth factor receptor: Role in human cancer. *Indian Journal of Dental Research: Official Publication of Indian Society for Dental Research* 2017; 28(6): 687-694.

[40] Lin HY, Zhao Y, Yu JN, et al. Effects of traditional Chinese medicine Wei-Wei-Kang-Granule on the expression of EGFR and NF-KB in chronic atrophic gastritis rats. *African Journal of Traditional, Complementary, and Alternative Medicines: AJTCAM* 2012; 9(1): 1-7.

[41] Chen X, Wang R, Bao C, et al. Palmatine ameliorates Helicobacter pylori-induced chronic atrophic gastritis by inhibiting MMP-10 through ADAM17/EGFR. *European Journal of Pharmacology* 2020; 882: 173267.

[42] Darnell JE, Jr. STATs and gene regulation. *Science* 1997; 277(5332): 1630-1635.

[43] Loh CY, Arya A, Naema AF, et al. Signal Transducer and Activator of Transcription (STATs) Proteins in Cancer and Inflammation: Functions and Therapeutic Implication. *Frontiers in Oncology* 2019; 9: 48.

[44] Ishii Y, Shibata W, Sugimori M, et al. Activation of Signal Transduction and Activator of Transcription 3 Signaling Contributes to Helicobacter-Associated Gastric Epithelial Proliferation and Inflammation. *Gastroenterology Research and Practice* 2018; 2018: 9050715.

[45] Hu Y, Zeng T, Xiao Z, et al. Immunological role and underlying mechanisms of B7-H6 in tumorigenesis. *Clinica Chimica Acta; International Journal of Clinical Chemistry* 2020; 502: 191-198.

[46] Goldar S, Khaniani MS, Derakhshan SM, et al. Molecular mechanisms of apoptosis and roles in cancer development and treatment. *Asian Pacific Journal of Cancer Prevention: APJCP* 2015; 16(6): 2129-2144.

[47] Xia HH, Talley NJ. Apoptosis in gastric epithelium induced by Helicobacter pylori infection: implications in gastric carcinogenesis. *American Journal of Gastroenterology* 2001; 96(1): 16-26.